^{18}F-FDG PET/CT for Target Volume Contouring in Lung Cancer Radiotherapy

Martin Stuschke and Christoph Pöttgen

Department of Radiotherapy, University Hospital Essen, University of Duisburg-Essen, Essen, Germany

In 2005, Nestle et al. (*1*) published their seminal paper comparing different methods to delineate radiotherapy target volume from ^{18}F-FDG PET in non–small cell lung cancer (NSCLC). They compared 4 different methods for primary delineation of gross-tumor target volume: a visual method, 2 fixed-threshold methods, and 1 adaptive-threshold method. They found that the corresponding gross-tumor target volumes differ considerably and that the more complex adaptive-threshold algorithm should be further evaluated. From these early steps of evaluation, the randomized PET-Plan multicenter trial was developed to compare locoregional progression after definitive radiochemotherapy using ^{18}F-FDG PET–based planning target volumes or conventional planning target volumes in locally advanced NSCLC (*2*). The PET-based gross tumor target volumes were delineated with a semiautomatic adaptive-threshold algorithm and expanded to clinical target volumes, including the anatomic extent of involved lymph nodes, and to a planning target volume that also considered set-up errors. The conventional target volumes contained the PET-based target volumes but included parts of PET-negative tumor-associated atelectases, as well as elective mediastinal nodal volumes known to be at higher risk from surgical series. Slightly higher total radiation doses were given in the PET-based arm respecting predefined normal-tissue tolerances. Noninferiority of the PET-based planning target volumes could be confirmed in a per-protocol analysis. The PET-Plan trial took more than 10 years from the initial methodologic studies in 2005 until publication in 2020, indicating the prolonged innovation cycles needed to establish new methods with high-level evidence in radiation

Received Jun. 15, 2020; revision accepted Aug. 27, 2020.
For correspondence or reprints contact: Martin Stuschke, University of Duisburg-Essen Medical School, Hufelandstrasse 55, Essen, 45122 Germany.
E-mail: martin.stuschke@uk-essen.de

DOI: 10.2967/jnumed.120.251660

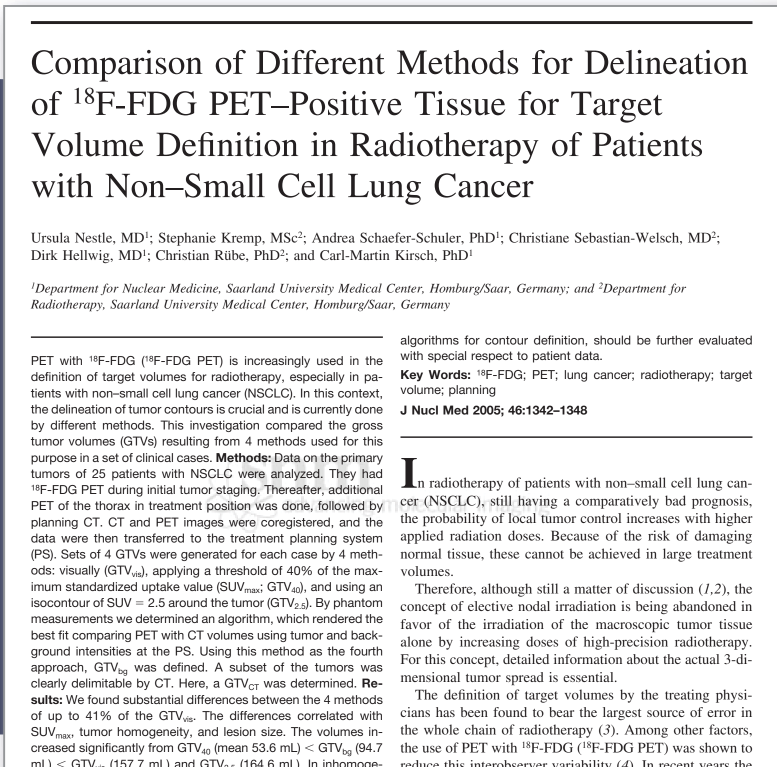

Comparison of Different Methods for Delineation of ^{18}F-FDG PET–Positive Tissue for Target Volume Definition in Radiotherapy of Patients with Non–Small Cell Lung Cancer

Ursula Nestle, MD[1]; Stephanie Kremp, MSc[2]; Andrea Schaefer-Schuler, PhD[1]; Christiane Sebastian-Welsch, MD[2]; Dirk Hellwig, MD[1]; Christian Rübe, PhD[2]; and Carl-Martin Kirsch, PhD[1]

[1]Department for Nuclear Medicine, Saarland University Medical Center, Homburg/Saar, Germany; and [2]Department for Radiotherapy, Saarland University Medical Center, Homburg/Saar, Germany

PET with ^{18}F-FDG (^{18}F-FDG PET) is increasingly used in the definition of target volumes for radiotherapy, especially in patients with non–small cell lung cancer (NSCLC). In this context, the delineation of tumor contours is crucial and is currently done by different methods. This investigation compared the gross tumor volumes (GTVs) resulting from 4 methods used for this purpose in a set of clinical cases. **Methods:** Data on the primary tumors of 25 patients with NSCLC were analyzed. They had ^{18}F-FDG PET during initial tumor staging. Thereafter, additional PET of the thorax in treatment position was done, followed by planning CT. CT and PET images were coregistered, and the data were then transferred to the treatment planning system (PS). Sets of 4 GTVs were generated for each case by 4 methods: visually (GTV_{vis}), applying a threshold of 40% of the maximum standardized uptake value (SUV_{max}; GTV_{40}), and using an isocontour of SUV = 2.5 around the tumor ($GTV_{2.5}$). By phantom measurements we determined an algorithm, which rendered the best fit comparing PET with CT volumes using tumor and background intensities at the PS. Using this method as the fourth approach, GTV_{bg} was defined. A subset of the tumors was clearly delimitable by CT. Here, a GTV_{CT} was determined. **Results:** We found substantial differences between the 4 methods of up to 41% of the GTV_{vis}. The differences correlated with SUV_{max}, tumor homogeneity, and lesion size. The volumes increased significantly from GTV_{40} (mean 53.6 mL) < GTV_{bg} (94.7 mL) < GTV_{vis} (157.7 mL) and $GTV_{2.5}$ (164.6 mL). In inhomoge- algorithms for contour definition, should be further evaluated with special respect to patient data.

Key Words: ^{18}F-FDG; PET; lung cancer; radiotherapy; target volume; planning

J Nucl Med 2005; 46:1342–1348

In radiotherapy of patients with non–small cell lung cancer (NSCLC), still having a comparatively bad prognosis, the probability of local tumor control increases with higher applied radiation doses. Because of the risk of damaging normal tissue, these cannot be achieved in large treatment volumes.

Therefore, although still a matter of discussion (*1,2*), the concept of elective nodal irradiation is being abandoned in favor of the irradiation of the macroscopic tumor tissue alone by increasing doses of high-precision radiotherapy. For this concept, detailed information about the actual 3-dimensional tumor spread is essential.

The definition of target volumes by the treating physicians has been found to bear the largest source of error in the whole chain of radiotherapy (*3*). Among other factors, the use of PET with ^{18}F-FDG (^{18}F-FDG PET) was shown to reduce this interobserver variability (*4*). In recent years the

oncology (*2*). The PET-Plan and other trials showed that only about 20% of locoregional recurrences were outside the PET-based target volume and that the relapses at the initial PET-positive macroscopic tumor and at distant metastases remain the dominant risks after the radiochemotherapy regimens used. Therefore, the sensitivity of ^{18}F-FDG PET/CT turned out to be good enough for target volume delineation of locally advanced NSCLC given the concurrent risks of in-field locoregional relapse and distant metastases. Subclinical regional disease not detected by PET/CT might not be of critical relevance for these treatment regimes.

In delineating target volumes, it is of special importance that tumor motion be separated from anatomic tumor spread, as motion during radiation therapy can be selectively reduced by gating or tracking or by irradiation during voluntary breath-hold. Important new techniques emerge in clinical routine, such as elastic motion deblurring algorithms for calculation of motion-corrected images with improved lesion contrast. In addition, advanced automatic segmentation algorithms on PET/CT are under evaluation using deep-learning methods.

^{18}F-FDG PET/CT has additional great benefits for radiotherapy planning in stage III NSCLC. The prognosis of patients with locally advanced NSCLC was improved during the first decade of this century, mainly not because of development of more effective treatments but because of stage migration due to the increased sensitivity of ^{18}F-FDG PET/CT for detection of distant metastases (*3*).

Decreases in SUV in the primary tumor during induction chemotherapy could be validated as an important prognostic factor for survival and progression-free survival after radiochemotherapy in NSCLC (*4*). Dose escalation strategies on tumor with residual metabolic activity in a midtreatment ^{18}F-FDG PET/CT study are under investigation for patients with locally advanced NSCLC, as in the RTOG1106/ACRIN 6697 trial, but mature data are lacking (*5*).

In conclusion, the work of Nestle et al. pioneered ^{18}F-FDG PET–based target volume segmentation in radiotherapy of locally advanced NSCLC, allowing omission of elective nodal irradiation. Improving the accuracy of the target volumes in radiotherapy by integrating the latest technical achievements and thorough validation remains a central task in radiotherapy.

DISCLOSURE

No potential conflict of interest relevant to this article was reported.

REFERENCES

1. Nestle U, Kremp S, Schaefer-Schuler A, et al. Comparison of different methods for delineation of ^{18}F-FDG PET–positive tissue for target volume definition in radiotherapy of patients with non–small cell lung cancer. *J Nucl Med*. 2005;46: 1342–1348.
2. Nestle U, Schimek-Jasch T, Kremp S, et al. Imaging-based target volume reduction in chemoradiotherapy for locally advanced non-small-cell lung cancer (PET-Plan): a multicentre, open-label, randomised, controlled trial. *Lancet Oncol*. 2020;21:581–592.
3. Chee KG, Nguyen DV, Brown M, et al. Positron emission tomography and improved survival in patients with lung cancer: the Will Rogers phenomenon revisited. *Arch Intern Med*. 2008;168:1541–1549.
4. Pöttgen C, Gauler T, Bellendorf A, et al. Standardized uptake decrease on [^{18}F]-fluorodeoxyglucose positron emission tomography after neoadjuvant chemotherapy is a prognostic classifier for long-term outcome after multimodality treatment: secondary analysis of a randomized trial for resectable stage IIIA/B non-small-cell lung cancer. *J Clin Oncol*. 2016;34:2526–2533.
5. Kong F-M, Ten Haken RK, Schipper M, et al. Effect of midtreatment PET/CT adapted radiation therapy with concurrent chemotherapy in patients with locally advanced non-small-cell lung cancer: a phase 2 clinical trial. *JAMA Oncol*. 2017; 3: 1358–1365.

Comparison of Different Methods for Delineation of ^{18}F-FDG PET–Positive Tissue for Target Volume Definition in Radiotherapy of Patients with Non–Small Cell Lung Cancer

Ursula Nestle, MD[1], Stephanie Kremp, MSc[2], Andrea Schaefer-Schuler, PhD[1], Christiane Sebastian-Welsch, MD[2], Dirk Hellwig, MD[1], Christian Rube, PhD[2], and Carl-Martin Kirsch, PhD[1]

[1]Department for Nuclear Medicine, Saarland University Medical Center, Homburg/Saar, Germany; and [2]Department for Radiotherapy, Saarland University Medical Center, Homburg/Saar, Germany

PET with ^{18}F-FDG (^{18}F-FDG PET) is increasingly used in the definition of target volumes for radiotherapy, especially in patients with non-small cell lung cancer (NSCLC). In this context, the delineation of tumor contours is crucial and is currently done by different methods. This investigation compared the gross tumor volumes (GTVs) resulting from 4 methods used for this purpose in a set of clinical cases. **Methods:** Data on the primary tumors of 25 patients with NSCLC were analyzed. They had ^{18}F-FDG PET during initial tumor staging. Thereafter, additional PET of the thorax in treatment position was done, followed by planning CT. CT and PET images were coregistered, and the data were then transferred to the treatment planning system (PS). Sets of 4 GTVs were generated for each case by 4 methods: visually (GTV_{vis}), applying a threshold of 40% of the maximum standardized uptake value (SUV_{max}; GTV_{40}), and using an isocontour of SUV = 2.5 around the tumor ($GTV_{2.5}$). By phantom measurements we determined an algorithm, which rendered the best fit comparing PET with CT volumes using tumor and background intensities at the PS. Using this method as the fourth approach, $GTV_{bg}$was defined. A subset of the tumors was clearly delimitable by CT. Here, a $GTV_{ct}$was determined. **Results:** We found substantial differences between the 4 methods of up to 41% of the GTV_{vis}. The differences correlated with SUV_{max}, tumor homogeneity, and lesion size. The volumes increased significantly from GTV_{40} (mean 53.6 mL) < GTV_{bg} (94.7 mL) < GTV_{vis} (157.7 mL) and GTV_{25} (164.6 mL). In inhomogeneous lesions, GTV_{40} led to visually inadequate tumor coverage in 3 of 8 patients, whereas GTV_{bg} led to intermediate, more satisfactory volumes. In contrast to all other GTVs, GTV_{40} did not correlate with the GTV_{CT}. **Conclusion:** The different techniques of tumor contour definition by ^{18}F-FDG PET in radiotherapy planning lead to substantially different volumes, especially in patients with inhomogeneous tumors. Here, the GTV_{40} does not appear to be suitable for target volume delineation. More complex methods, such as system-specific contrast-oriented algorithms for contour definition, should be further evaluated with special respect to patient data.

Key Words: ^{18}F-FDG; PET; lung cancer; radiotherapy; target volume; planning

J Nucl Med 2005; 46:1342–1348
DOI: 10.2967/jnumed.120.251660a

In radiotherapy of patients with non-small cell lung cancer (NSCLC), still having a comparatively bad prognosis, the probability of local tumor control increases with higher applied radiation doses. Because of the risk of damaging normal tissue, these cannot be achieved in large treatment volumes.

Therefore, although still a matter of discussion (*1,2*), the concept of elective nodal irradiation is being abandoned in favor of the irradiation of the macroscopic tumor tissue alone by increasing doses of high-precision radiotherapy. For this concept, detailed information about the actual 3-dimensional tumor spread is essential.

The definition of target volumes by the treating physicians has been found to bear the largest source of error in the whole chain of radiotherapy (*3*). Among other factors, the use of PET with ^{18}F-FDG (^{18}F-FDG PET) was shown to reduce this interobserver variability (*4*). In recent years the possibly high impact of ^{18}F-FDG PET on the size and form of target volumes in lung cancer was demonstrated (*5–10*).

In diagnostic nuclear medicine, extensive research on F-FDG PET was conducted, mostly dealing with diagnostic performance—for example, the determination of standardized uptake values (SUVs) (*11–14*). Neither the lesion size nor the localization of the tumor contour played an important role in these investigations.

However, these factors are directly linked to the size and shape of target volumes and, therefore, crucial for radiotherapy planning.

Various methods are currently used to determine the outline of ^{18}F-FDG-positive tissue. The first one applied (*5,7*), and still widely used, is the visual interpretation of the PET scan and the definition of contours as judged by the experienced nuclear medicine physician.

Other methods attempt to find a threshold for image segmentation: In diagnostic studies, a maximum SUV (SUV_{max}) of 2.5 is often defined and still discussed as a threshold for the distinction between malignant and benign lesions. Although aimed at the characterization of a point of most intense ^{18}F-FDG accumulation within a questionable lesion, this value was also suggested as a threshold for gross tumor volume (GTV) delineation (*15*).

From the physics side, after phantom studies (*16,17*), thresholding by percentage (e.g., 40% or 50%) of the maximum uptake was done (*4,8,18–20*). Recently, more complex algorithms—including, for example, the source-to-background ratio or local contrast—were proposed (*21,22*).

Today, all these philosophies are applied simultaneously by different groups active in this field. To our knowledge, no comparison of the resulting volumes and quantification of possible

Received Jan. 21, 2005; revision accepted Apr. 13, 2005.
For correspondence contact: Ursula Nestle, MD, Klinik für Nuklearmedizin, Universitätsklinikum des Saarlandes, D-66421 Homburg/Saar, Germany.
E-mail: raunes@uniklinik-saarland.de

differences were performed in patient data. This was the aim of the present investigation.

MATERIALS AND METHODS

Data of 25 patients with histologically proven primary NSCLC were used, who had a routine ^{18}F-FDG PET examination for staging purposes. All patients had an option for radiotherapy at the time of the PET examination, although not all patients finally received this treatment.

Tumor stages were T1 or T2 in 17 patients and T3 or T4 in 8 patients. Eighteen patients had positive mediastinal nodes; 6 patients had distant metastases.

Our investigation focuses on the GTVs concerning the primary tumors, regardless of the N and M stages.

After obtaining informed consent, patients underwent routine whole-body ^{18}F-FDG PET (250 MBq ^{18}F-FDG; fasting blood glucose level, <150 mg/dL; CTI/Siemens ECAT ART PET scanner; 6 or 7 bed positions; attenuation correction by transmission scanning with ^{137}Cs single-photon transmission; axial spacing 3.4 mm; iterative reconstruction into 128 × 128 pixels of 5.1 mm), with the acquisition being started 90 min after injection. Afterward (160 min after injection), an additional PET scan of the chest was acquired in radiotherapy treatment position (2 or 3 bed positions). On the same day, spiral planning CT of the chest (El-Scint TWIN FLASH CT; 3-mm slice thickness, 512 × 512 pixels of 0.98 mm, flat breathing) was performed in identical position verified by laser localizer, skin marks, and photographic documentation. The coregistration of CT and PET data (*23*) was performed by a Hermes (Nuclear Diagnostics) workstation; the data were then transferred to the radiotherapy planning system (Philips Pinnacle).

As a first step, in all patients, an experienced double board-certified nuclear medicine and radiotherapy physician used the region-of-interest (ROI) standard evaluation tool provided by the manufacturer of the PET system and a global logarithmic scaling to generate a "visual" PET GTV, comprising the tissue considered visually as part of the malignant primary tumor (GTV_{vis}). Clinical information and CT reports of the patients were used in this process but CT images or image fusion was not used.

Then, for all tumors, 2 further GTVs were defined at the PET console. ROIs were positioned around the tumors slice by slice in the volume file, using first an isocontour of SUV = 2.5 ($GTV_{2.5}$) and, second, an isocontour of 40% of the SUV_{max} of the whole lesion (GTV_{40}) similarly for all slices.

In our opinion, the radiotherapy planning system (PS) is the most likely place for PET target volumes to be defined in clinical practice. The data transfer described converts the voxel values of PET activity (kBq/mL) to visual intensities (I), so that the SUV is lost. Furthermore, the matrix is changed from 128 × 128 to 512 × 512. Therefore, the delineation of the fourth set of GTVs was done on the PS using an in-house algorithm.

As reported earlier in part (*24*), in-house phantom measurements were performed using spheres with varying diameters and source-to-background activities.

The physical and mathematic features and results of these phantom experiments will be published separately in more detail. However, the clinical application of the resulting algorithm was included into our comparison.

In short, by means of the PS, thresholds for volume contouring are determined by a function of tumor and background intensities:

$$I_{threshold} = (0.15 \times I_{mean}) + I_{background}.$$

In patient datasets, I_{mean} was calculated as the mean intensity of all pixels surrounded by the 70% Imax isocontour within the tumor. The rationale for the choice of I_{mean} rather than I_{max} was to minimize the influence of statistically not representative maximum values on the resulting threshold.

$I_{background}$ was defined as follows: Anatomic entities adjacent to the tumor (e.g., lung, mediastinum, liver) were identified. By visual comparison of these, the structure with the highest ^{18}F-FDG uptake was defined as "relevant backround." A ROI was placed into the relevant background structure at a safe distance from the target, and the mean SUV of this ROI was used as $I_{background}$ for threshold calculation. This procedure was established on the assumption that, for tumors adjacent to various anatomic structures, those with more intense ^{18}F-FDG accumulation after injection (e.g., mediastinum, liver) were more relevant for threshold calculation than faintly accumulating tissue (e.g., lung). We further assumed, and confirmed this assumption by exploratory measurements, that normal organs show a rather homogeneous ^{18}F-FDG accumulation after injection within themselves.

Applying the resulting thresholds in the 22 patients eligible for evaluation at the PS (in 3 patients, data transfer failed because of technical reasons), tumor contours were outlined automatically and then manually corrected to exclude nontumor tissue—for example, myocardium. This procedure led to the fourth set of GTVs (GTV_{bg}).

As a common feature in lung cancer, in some cases ^{18}F-FDG-positive lymph nodes directly adjacent to the primary tumors could not be separated from the tumor itself. Here, the whole structure accumulating ^{18}F-FDG was included into all GTVs as if it was part of the primary tumor.

To correct for a possible influence of the tumor size on the differences detected, virtual spheric radii were calculated for all GTVs (R_{vis}, R_{40}, $R_{2.5}$, R_{bg}, R_{CT}). In addition, this yielded a value comparable to clinical practice, where the differences in radius would reflect the distance between the contours drawn in the same image.

In CT, as common in lung cancer, in most tumors the circumferences could only be partially contoured unequivocally. However, in 5 patients, a peripheral tumor was fully delimitable. Here a GTV derived from CT was generated using the soft-tissue window with respect to lung window (GTV_{CT}). To correct for breathing excursions during the PET scan, and therefore to provide a measure for the size of PET GTVs to be expected, "expanded CT volumes" were calculated (GTV_{CTexp}). Following the lower levels of tumor movements reported, and of correction margins recommended in the literature for radiotherapy planning (*25–28*), the expansion was 0.15 cm lateral, 0.2 cm anteroposterior, and 0.3 cm craniocaudal. Radius values derived from the unexpanded CT volumes were "expanded" by 0.25 cm.

By means of visual characterization of the ^{18}F-FDG accumulation, the tumors were classified as "rather homogeneous" or "grossly inhomogeneous."

The results were evaluated by standard methods of descriptive statistics, including combined *t* test and the Pearson correlation.

RESULTS

The SUV_{max} values of the primary tumors were in mean 17.1 (range, 1.7–38.7). As expected (*29*), this value was significantly higher compared with the whole-body examinations 90 min after injection (mean SUV_{max}, 13.4; $P < 0.0001$). However, 3 patients showed a decrease of SUV_{max}. One of these had the overall minimum SUV_{max} of 1.7 after an initial value of 3.6. Because the patient had a malignant lesion, later confirmed histologically, we decided to include this case as far as possible into the present investigation. However, no $GTV_{2.5}$ could be determined.

Table 1 shows the results with respect to volumes and spheric radii of the GTVs created as well as the results of the statistical comparison. Mean GTV_{vis} was 157.7 mL, representing a R_{vis} of

TABLE 1
Results of GTV Delineation Following Different Philosophies for Contour Definition: All Patients

		GTV_{vis}		$GTV_{2.5}$		GTV_{40}		GTV_{bg}	
	SUV_{max}	25		24		25		22	
n	25	Volume (mL)	Radius* (cm)	Volume (mL)	Radius* (cm)	Volume (mL)	Radius* (cm)	Volume (mL)	Radius* (cm)
Mean	17.1	157.7	3.03	164.6	3.05	53.6	2.18	94.7	2.52
Median	17.2	107.8	2.95	108.3	2.96	41.4	2.15	62.2	2.45
Maximum	38.8	666.2	5.42	655.7	5.39	168.3	3.42	318.0	4.23
Minimum	1.7	9.3	1.30	8.1	1.24	5.7	1.11	3.7	0.96
t test vs. GTV_{vis}		—		NS	NS	$P = 0.0004$	$P < 0.0001$	$P = 0.0002$	$p < 0.0001$
t test vs. $GTV_{2.5}$		—		—		$P = 0.0007$	$P < 0.0001$	$P = 0.0006$	$p < 0.0001$
t test vs. GTV_{40}		—		—	—	—	—	$P = 0.01$	$P = 0.006$

*Radius values were calculated from volumes as spheric radii.

3.03 cm. As can be seen, there are clear differences between the GTVs created. While the differences between GTV_{vis} and $GTV_{2\cdot5}$ appear rather small, all other differences were equal to or larger than the spatial resolution of the PET system. Despite the small group of patients examined, this was statistically highly significant.

The maximum difference in radius detected in an individual patient was 2.22 cm ($R_{vis} - R_{40}$), 41% of R_{vis} of this tumor.

The differences between GTV_{vis} and $GTV_{2.5}$ compared with GTV_{40} or GTV_{bg} correlated significantly with the SUV_{max}, the size of the lesion, and the presence of gross inhomogeneity (all P values < 0.01).

On further examination of these findings, 2 subgroups were analyzed exploratively:

In 8 patients, the tumors showed a grossly inhomogeneous ^{18}F-FDG accumulation. These tumors (Table 2) were significantly larger than the others (mean $R_{vis} = 4.16$ vs. 3.03 cm; $P < 0.0001$). However, they did not show a significantly different SUV_{max} (mean, 17.1 vs. 19.7; not significant [NS]).

In this group, the differences were as before but were more pronounced. Furthermore, by visual impression, in at least 3 of the 8 patients, there was grossly inadequate coverage of the malignant tissue by the GTV_{40} (Figs. 1 and 2), whereas GTV_{bg} proposed a better concordance of the ^{18}F-FDG accumulation with the lesions depicted by CT. The 5 tumors, which were fully delimitable by CT (Table. 3), were all located peripherally and, on average, smaller than those of the whole group examined (mean $GTV_{vis} = 66.5$ mL). The differences between the GTVs here were less pronounced than seen before (Fig. 3).

Despite the small number of cases, the GTV_{vis}, $GTV_{2.5}$, and GTV_{bg} values correlated clearly with GTV_{CT} (correlation

TABLE 2
Results of GTV Delineation Following Different Philosophies for Contour Definition: Patients with Grossly Inhomogeneous ^{18}F-FDG Accumulation

		GTV_{vis}		$GTV_{2.5}$		GTV_{40}		GTV_{bg}	
Patient no.	SUV_{max}	Volume (mL)	Radius* (cm)	Volume (mL)	Radius* (cm)	Volume (mL)	Radius* (cm)	Volume (mL)	Radius (cm)
1	20.1	467.7	4.82	494.0	4.90	96.8	2.85	264	3.98
6	23.8	666.2	5.42	655.7	5.39	136.5	3.19	318	4.23
8	20.4	223.9	3.77	188.9	3.56	97.6	2.86	137	3.20
10	11.9	159.8	3.37	107.0	2.94	52.5	2.32	73.8	2.60
13	19.5	375.0	4.47	428.9	4.68	69.2	2.55	280	4.06
14	15.9	182.7	3.52	271.4	4.02	111.8	2.99	112	2.99
22	22.4	176.2	3.48	179.5	3.50	53.1	2.33	97.9	2.86
23	23.7	371.3	4.46	377.5	4.48	168.3	3.43	239	3.85
Mean	19.7	327.9	4.16	337.9	4.18	98.2	2.81	190.2	3.47

*Radius values were calculated from volumes as spheric radii.

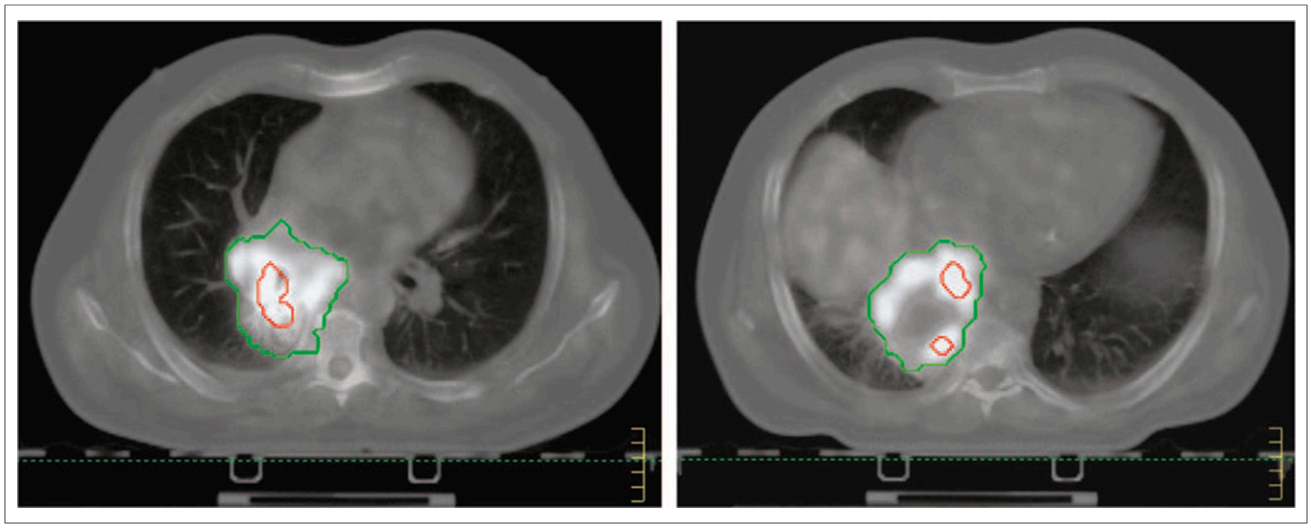

FIGURE 1. Two slices of image fusion in patient 1 with inadequate tumor coverage by GTV_{40} (red) in ^{18}F-FDG–inhomogeneous tumor (green = outline of GTV_{bg}).

coefficient = 0.96–0.98; all P values $\leq$ 0.02), whereas the GTV_{40} did not (correlation coefficient, 0.70; P = NS). However, because of the small number of cases, this result must be regarded with caution, and further statistical evaluation was not done.

DISCUSSION

The present investigation attempts to contribute to the discussion about the standardization of target volumes in radiotherapy planning as derived from ^{18}F-FDG PET. Though there are numerous investigations on phantom measurements addressing this problem, only a small number of studies including patient data have been published (*16,17,30*). To our knowledge, there is no clinical investigation on the potential differences between the various approaches.

Our study addressed this question by investigating the primary tumors of patients with NSCLC. Because of substantial anatomic and pathohistologic differences between primary tumors and lymph nodes, we believed that these should be dealt with separately.

Primarily, the aim of our investigation was to detect and quantify any differences between the delineation philosophies for ^{18}F-FDG PET. During this comparison, we perceived the need to determine the "true" volumes of the lesions investigated. However, for patient data—in contrast to phantom measurements—there is no golden standard for the evaluation of volumes as measured by different imaging modalities except pathologic specimens, which were not available because of the nature of our patient population. Furthermore, in lung tumors, results of in situ volumetry will always be dependent on how the individual method deals with tumor motion. Despite blurring, volumes of chest tumors as measured by ^{18}F-FDG PET (representing the accumulation averaged over several breathing cycles) would be expected to be equal or larger than the volumes as measured by CT, representing rather a "snapshot" of the density at one point of time during the breathing cycle (*28*). We therefore calculated "expanded" CT volumes according to the smallest margins recommended (*25–28*) for motion correction in radiotherapy planning

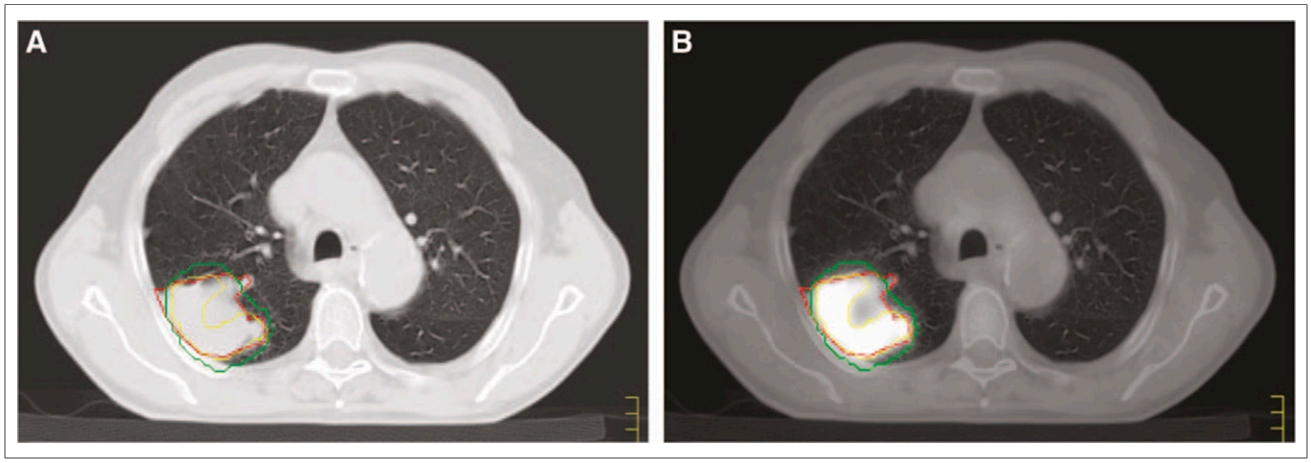

FIGURE 2. Planning CT scan (A) and corresponding fusion image (B) of patient 8 show inadequacy of GTV_{40}: green = GTV_{bg}, red = GTV_{CT}, yellow = GTV_{40}.

TABLE 3
Results of GTV Delineation Following Different Philosophies for Contour Definition: Patients with Clearly CT-Defined Tumors

Patient no.	SUV_{max}	GTV_{vis}		$GTV_{2.5}$		GTV_{40}		GTV_{bg}		GTV_{CT}		GTV_{CTexp}	
		Volume (mL)	Radius* (cm)	Volume (mL)	Radius* (cm)	Volume (mL)	Radius* (cm)	Volume (mL)	Radius* (cm)	Volume (mL)	Radius* (cm)	Volume (mL)	Radius* (cm)
4	30.1	164.2	3.40	151.1	3.30	56.2	2.38	82.0	2.70	66.4	2.51	109.0	2.76
5	6.1	39.2	2.11	30.0	1.93	41.4	2.15	12.4	1.44	12.1	1.42	25.9	1.67
7	1.7	9.3	1.3	—	—	5.7	1.11	3.7	0.96	5.5	1.1	17.0	1.6
9	17.2	52.3	2.32	35.5	2.04	14.1	1.50	21.4	1.72	12.7	1.45	19.5	1.70
16	18.3	67.8	2.53	42.7	2.17	13.2	1.47	23.1	1.77	32.0	1.97	55.3	2.22
Mean	14.7	66.5	2.33	64.8	2.36	26.1	1.72	28.5	1.72	25.7	1.69	44.6	1.94

*Radius values were calculated from volumes as spheric radii.

for tumors clearly delimitable by CT. To us, these expanded volumes appeared to be closest to the true PET volumes to be expected. For the other tumors, which—as frequently observed in lung cancer—were not fully delimitable, and, therefore, for which no CT volume could be determined, we compared the PET GTVs visually to CT findings in fusion images. As illustrated in Figures 1 and 2, even in tumors that are not fully delimitable, it can at least be determined whether or not a mass is roughly surrounded by an isocontour.

In the overall comparison of the 4 philosophies of contour definition, we found significant differences between the resulting target volumes. These differences correlated with SUV_{max}, lesion size, and tumor inhomogeneity.

Visual definition and the application of a constant isocontour of SUV = 2.5 rendered surprisingly similar results. No differences exceeding the spatial resolution of the PET scan were observed between these 2 methods. However, visual judgment is very much dependent on the individual investigator and display window setting—for example, the type of gray scale applied. Furthermore, the GTVs generated by these approaches appeared rather large in comparison with expanded CT data. Exploratory results on mediastinal lymph nodes have further shown us that, for faintly accumulating structures in a background with relatively high activity, the SUV = 2.5 isocontours are not suitable for target volume delineation.

The most striking findings of this study relate to the 40% SUV_{max} approach, which, in general, yielded the smallest set of GTVs. The differences in comparison with the visual or the $SUV_{2.5}$ approach were found to be larger than the resolution of the PET system.

In patients with inhomogeneous tumors, we observed a 3.6-fold difference in mean volume (GTV_{25} – GTV_{40}), corresponding to differences in radius up to 2.2 cm. In 3 of 8 patients, the visual impression of inadequate coverage of the malignant tissue by the 40% isocontour was obvious (Figs. 1 and 2).

In the tumors fully delimitable by CT, there was no correlation of GTV_{40} with GTV_{CT}, though this was the case for all other concepts.

The mean GTV_{40} in the present investigation was in the range of GTV_{CT} without expansion in well-delineated tumors, which were relatively small and situated peripherally. This finding is in line with the data by Erdi et al. (*16*), who used the 40% approach for GTV delineation. This group has meanwhile developed systems of breath control to be used for planning and irradiation (*9,31*), thus avoiding the problem of incongruent imaging of tumor

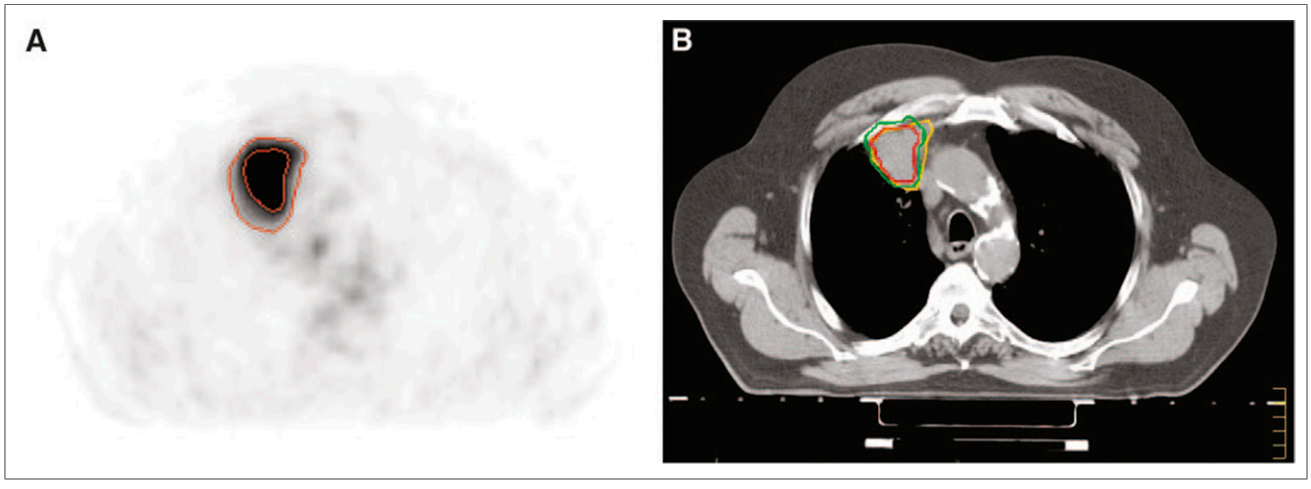

FIGURE 3. Example of difference between target volumes in patient 4 with a tumor clearly delimitable by CT. (A) ^{18}F-FDG PET. SUV_{max} = 30. Isocontours: narrow = GTV_{40}, wide = $GTV_{2.5}$. (B) Corresponding planning CT. Isocontours: red = GTV_{40}, green = GTV_{bg}, yellow = GTV_{CT}.

motion. However, if breath control is not applied, "tailoring down" CT-defined GTVs to PET contours generated by an automatic 40% SUV approach in lung cancer does not safely lead to a complete coverage of the malignant tissue.

The philosophy of defining target volume contours by an algorithm with respect to local background was proposed by several authors (*17,21*). One group even showed superiority of the ^{18}F-FDG PET volumes defined by a source-to-back-ground algorithm over CT- and MRI-measured volumes when compared with histologic specimens in larynx tumors (*30*).

The algorithm developed in our institution, to be used in the PS to define the threshold for the PET-positive volume as a function of the intensities of tumor and background, led to volumes (GTV_{bg}) of an intermediate size between the GTV_{25} and the GTV_{40}. In visual comparison with CT data, these volumes seemed to fit pathoanatomic structures better than the GTV_{40}.

The GTV_{bg} algorithm is closely related to the departmental setup. The exploratory use of the formula for volume definition away from the PS—for example, at the PET system itself—led to significantly different volumes. It must be pointed out that technical and software factors of all steps involved do have an important influence on the structure of image data and on resulting volumes. Therefore, any contouring algorithm must be regarded as system specific for use at the point of the radiotherapy chain for which it was developed. As with all other parts of the radiotherapy chain, PET contouring algorithms must be quality controlled for each system, including phantom measurements, before being used in any application.

The GTV_{bg} method, however, appears to be more stable against the inhomogeneity of tumor uptake, and the broad variation of SUV_{max} values between patients, than, for example, the 40% approach.

An important issue to be discussed before the use of complex algorithms in radiotherapy planning for lung cancer is the choice of the "relevant" background. Until now, most publications in this context have been phantom studies (*21,22*) so that the current literature does not provide solutions for this problem. To our knowledge, the only investigation published to date on the use of a source-to-back-ground algorithm in patients (*30*) focused on larynx tumors. In the head-and-neck region, the differences in normal tissue accumulation are not as high as in the thorax. In the chest, mean ^{18}F-FDG uptake in normal tissues may vary between a SUV of <1 (lung) up to a SUV of >3 (liver). Depending on the algorithm used, these differences may lead to significantly different thresholds, especially in contouring tumors with only faint accumulation of ^{18}F-FDG. For the present investigation we used a differentiated approach, choosing and measuring the relevant background as defined for each patient separately, with the encouraging results reported.

A possible limitation of the present investigation might be found in the late acquisition of the planning PET scans. Other groups have reported on PET scans acquired much earlier after injection (e.g., 45–60 min). It is known that the ^{18}F-FDG uptake in malignant tumors rises over time, though decreasing in other tissues (*29,32,33*). This may possibly lead to an accentuation of our findings. However, exploratory delineation of GTVs both in early and in late PET scans of several patients did not show relevant changes of the results.

Overall, there is a great need for imaging methods that precisely depict tumor tissue to aid the delineation of target volumes in high-dose 3-dimensional irradiation. Because of the high image contrast, and the comparably high diagnostic accuracy, ^{18}F-FDG PET has a large potential in this context, which urgently needs to be integrated into clinical trials.

A first prospective study has already shown that the probability of local tumor recurrence outside the planning target volume is low after irradiating only the ^{18}F-FDG–positive tissue (*34*). It is clear that patients with large—and therefore inhomogeneous—tumors might benefit from dose escalation (*35*). Because the differences between the philosophies for target volume definition by ^{18}F-FDG PET aremost pronounced in this group of patients, the development of a standard for the delineation of ^{18}F-FDG-positive tissue is needed.

CONCLUSION

The different techniques used for tumor contour definition by ^{18}F-FDG PET in radiotherapy planning resulted in substantially different volumes, especially in patients with inhomogeneous tumors.

Because of possibly incomplete tumor coverage, to us, the 40% SUV_{max} concept does not appear generally suitable for target volume delineation unless systems are used for breath control.

More complex algorithms—for example, contrast-oriented methods for contour definition—should further be evaluated with special respect to patient data.

It must be emphasized that such algorithms are system specific and that the whole chain from the PET system to the treatment PS must strictly be quality controlled when used in clinical practice.

ACKNOWLEDGMENTS

The authors thank the staff of our departments as well as the colleagues from the Department of Pneumology for their close collaboration. Furthermore, we thank Andrew Page for his help in the wording of the manuscript.

REFERENCES

1. Armstrong JG. Target volume definition for three-dimensional conformal radiation therapy of lung cancer. *Br J Radiol.* 1998;71:587–594.
2. Nestle U, Hellwig D, Schmidt S, et al. 2-Deoxy-2-[^{18}F]fluoro-D-glucose positron emission tomography in target volume definition for radiotherapy of patients with non-small-cell lung cancer. *Mol Imaging Biol.* 2002;4:257–263.
3. Rasch C, Remeijer P, Koper PC, et al. Comparison of prostate cancer treatment in two institutions: a quality control study. *Int J Radiat Oncol Biol Phys.* 1999;45:1055–1062.
4. Mah K, Caldwell CB, Ung YC, et al. The impact of ^{18}FDG-PET on target and critical organs in CT-based treatment planning of patients with poorly defined non-small-cell lung carcinoma: a prospective study. *Int J Radiat Oncol Biol Phys.* 2002;52:339–350.
5. Nestle U, Walter K, Schmidt S, et al. ^{18}F-Deoxyglucose positron emission tomography (^{18}FDG-PET) for the planning of radiotherapy in lung cancer: high impact in patients with atelectasis. *Int J Radiat Oncol Biol Phys.* 1999;44:593–597.
6. Hebert ME, Lowe VJ, Hoffman JM, Patz EF, Anscher MS. Positron emission tomography in the pretreatment evaluation and follow-up of non-small cell lung cancer patients treated with radiotherapy: preliminary findings. *Am J Clin Oncol.* 1996;19:416–421.
7. Kiffer JD, Berlangieri SU, Scott AM, et al. The contribution of ^{18}F-fluoro-2-deoxy-glucose positron emission tomographic imaging to radiotherapy planning in lung cancer. *Lung Cancer.* 1998;19:167–177.
8. Bradley J, Thorstad WL, Mutic S, et al. Impact of ^{18}FDG-PET on radiation therapy volume delineation in non-small-cell lung cancer. *Int J Radiat Oncol Biol Phys.* 2004;59:78–86.
9. Erdi YE, Rosenzweig K, Erdi AK, et al. Radiotherapy treatment planning for patients with non-small cell lung cancer using positron emission tomography (PET). *Radiother Oncol.* 2002;62:51–60.
10. Vanuytsel LJ, Vansteenkiste JF, Stroobants SG, et al. The impact of ^{18}F-fluoro-2-deoxy-D-glucose positron emission tomography (FDG-PET) lymph node staging

on the radiation treatment volumes in patients with non-small cell lung cancer. *Radiother Oncol.* 2000;55:317–324.
11. Vansteenkiste J, Fischer BM, Dooms C, Mortensen J. Positron-emission tomography in prognostic and therapeutic assessment of lung cancer: systematic review. 35. *Lancet Oncol.* 2004;5:531–540.
12. Baum RP, Hellwig D, Mezzetti M. Position of nuclear medicine modalities in the diagnostic workup of cancer patients: lung cancer. *Q J Nucl Med Mol Imaging.* 2004;48:119–142.
13. Dwamena BA, Sonnad SS, Angobaldo JO, Wahl RL. Metastases from non-small cell lung cancer: mediastinal staging in the 1990s—meta-analytic comparison of PET and CT. *Radiology.* 1999;213:530–536.
14. Hellwig D, Ukena D, Paulsen F, Bamberg M, Kirsch CM. Meta-analysis of the efficacy of positron emission tomography with F-18-fluorodeoxyglucose in lung tumors: basis for discussion of the German Consensus Conference on PET in Oncology 2000. *Pneumologie.* 2001;55:367–377.
15. Paulino AC, Johnstone PA. FDG-PET in radiotherapy treatment planning: Pandora's box? *Int J Radiat Oncol Biol Phys.* 2004;59:4–5.
16. Erdi YE, Mawlawi O, Larson SM, et al. Segmentation of lung lesion volume by adaptive positron emission tomography image thresholding. *Cancer.* 1997; 80(suppl):2505–2509.
17. Ciernik IF, Dizendorf E, Baumert BG, et al. Radiation treatment planning with an integrated positron emission and computer tomography (PET/CT): a feasibility study. *Int J Radiat Oncol Biol Phys.* 2003;57:853–863.
18. Scarfone C, Lavely WC, Cmelak AJ, et al. Prospective feasibility trial of radiotherapy target definition for head and neck cancer using 3-dimensional PET and CT imaging. *J Nucl Med.* 2004;45:543–552.
19. Giraud P, Grahek D, Montravers F, et al. CT and ^{18}F-deoxyglucose (FDG) image fusion for optimization of conformal radiotherapy of lung cancers. *Int J Radiat Oncol Biol Phys.* 2001;49:1249–1257.
20. Miller TR, Grigsby PW. Measurement of tumor volume by PET to evaluate prognosis in patients with advanced cervical cancer treated by radiation therapy. *Int J Radiat Oncol Biol Phys.* 2002;53:353–359.
21. Black QC, Grills IS, Kestin LL, et al. Defining a radiotherapy target with positron emission tomography. *Int J Radiat Oncol Biol Phys.* 2004;60:1272–1282.
22. Daisne JF, Sibomana M, Bol A, Doumont T, Lonneux M, Gregoire V. Tridimensional automatic segmentation of PET volumes based on measured source-to-background ratios: influence of reconstruction algorithms. *Radiother Oncol.* 2003;69:247–250.
23. Kremp S, Hellwig D, Schaefer-Schuler A, Sebastian-Welsch C, Ukena D, Rube C. Integration of PET/CT fusion images into the 3-D conformal radiotherapy planning of lung cancer patients [in German] [abstract]. *Strahlenther Onkol.* 2003;179(suppl 1):6.
24. Kremp S, Schaefer-Schuler A, Nestle U, Sebastian-Welsch C, Rube C, Kirsch CM. Comparison of CT and CT-PET-fusion based 3D treatment plans in the percutaneous radiotherapy of lung cancer. *Radiother Oncol.* 2004;73(suppl 1): S447–S448.
25. Seppenwoolde Y, Shirato H, Kitamura K, et al. Precise and real-time measurement of the 3D tumor motion in lung due to breathing and heartbeat, measured during radiotherapy. *Int J Radiat Oncol Biol Phys.* 2002;53:822–834.
26. Stevens CW, Munden RF, Forster KM, et al. Respiratory-driven lung tumor motion is independent of tumor size, tumor location, and pulmonary function. *Int J Radiat Oncol Biol Phys.* 2001;51:62–68.
27. Hof H, Herfath K, Mlinter M, Essig M, Wannenmacher M, Debus J. The use of multislice-CT for the determination of respiratory lung tumor movement in stereotactic single-dose irradiation. *Strahlenther Onkol.* 2003;179:542–547.
28. Caldwell CB, Mah K, Skinner M, Danjoux CE. Can PET provide the 3D extent of tumor motion for individualized internal target volumes? A phantom study of the limitations of CT and the promise of PET. *Int J Radiat Oncol Biol Phys.* 2001;55:1381–1393.
29. Matthies A, Hickeson M, Cuchiara A, Alavi A. Dual time point 18-FDG-PET for the evaluation of pulmonary nodules. *J Nucl Med.* 2002;43:871–875.
30. Geets X, Daisne JF, Gregoire V, Harmoir M, Lonneux M. Role of 11-C-methionine positron emission tomography for the delineation of the tumor volume in pharyngolaryngeal squamous cell carcinoma: comparison with FDG-PET and CT. *Radiother Oncol.* 2004;71:267–273.
31. Nehmeh SA, Erdi YE, Ling CC, et al. Effect of respiratory gating on quantifying PET images of lung cancer. *J Nucl Med.* 2002;43:876–881.
32. Hamberg LM, Hunter GJ, Alpert NM, Choi NC, Babich JW, Fischman AJ. The dose uptake ratio as an index of glucose metabolism: useful parameter or oversimplification? *J Nucl Med.* 1993;35:1308–1312.
33. Yamada S, Kubota K, Kubota R, Ido T, Tamahashi N. High accumulation of fluorine-18-fluorodeoyxglucose in turpentine-induced inflammatory tissue. *J Nucl Med.* 1995;36:1301–1306.
34. De Ruysscher D, Wanders S, van Haren E, et al. Selective mediastinal node irradiation on the basis of the FDG-PET scan in patients with NSCLC is safe: results of a prospective clinical study. *Radiother Oncol.* 2004;73(suppl 1):S143–S135.
35. Rosenzweig KE, Amols H, Ling CC. New radiotherapy technologies. *Semin Surg Oncol.* 2003;21:190–195.